Asian Journal of Andrology (2020) 22, 169–176
www.asiaandro.com; www.ajandrology.com

Open Access

ORIGINAL ARTICLE

Sperm Biology

Mechanistic target of rapamycin kinase (*Mtor*) is required for spermatogonial proliferation and differentiation in mice

Jun Cao[1], Zuo-Bao Lin[2], Ming-Han Tong[1], Yong-Lian Zhang[1], Yi-Ping Li[2], Yu-Chuan Zhou[1]

Spermatogonial development is a vital prerequisite for spermatogenesis and male fertility. However, the exact mechanisms underlying the behavior of spermatogonia, including spermatogonial stem cell (SSC) self-renewal and spermatogonial proliferation and differentiation, are not fully understood. Recent studies demonstrated that the mTOR complex 1 (mTORC1) signaling pathway plays a crucial role in spermatogonial development, but whether MTOR itself was also involved in any specific process of spermatogonial development remained undetermined. In this study, we specifically deleted *Mtor* in male germ cells of mice using *Stra8*-Cre and assessed its effect on the function of spermatogonia. The *Mtor* knockout (KO) mice exhibited an age-dependent perturbation of testicular development and progressively lost germ cells and fertility with age. These age-related phenotypes were likely caused by a delayed initiation of *Mtor* deletion driven by *Stra8*-Cre. Further examination revealed a reduction of differentiating spermatogonia in *Mtor* KO mice, suggesting that spermatogonial differentiation was inhibited. Spermatogonial proliferation was also impaired in *Mtor* KO mice, leading to a diminished spermatogonial pool and total germ cell population. Our results show that MTOR plays a pivotal role in male fertility and is required for spermatogonial proliferation and differentiation.

Asian Journal of Andrology (2020) **22**, 169–176; doi: 10.4103/aja.aja_14_19; published online: 24 May 2019

Keywords: male fertility; mice; *Mtor*; spermatogenesis; spermatogonia; testis

INTRODUCTION

Spermatogenesis is a highly intricate and coordinated process that allows continuous daily production of millions of spermatozoa throughout the reproductive lifespan of male mammals.[1] This sustained production of spermatozoa depends on the development of spermatogonia, which was classified into two subpopulations, undifferentiated spermatogonia and differentiating spermatogonia.[2,3] In mice and other rodents, undifferentiated spermatogonia include spermatogonial stem cells (SSCs) and progenitor spermatogonia, which can be subdivided into A_{single} (A_s), A_{paired} (A_{pr}), and $A_{aligned}$ (A_{al}) spermatogonia according to the number of cells connected by intercellular cytoplasmic bridges. Differentiating spermatogonia are derived from undifferentiated spermatogonia and consist of A_1, A_2, A_3, A_4, intermediate (In), and Type B spermatogonia.[3–7] SSC self-renewal, spermatogonial proliferation, and spermatogonial differentiation are vital prerequisites for spermatogenesis. Self-renewal of SSC provides the foundation for the continuity of spermatogenesis. The initiation of spermatogenesis occurs when SSCs leave the self-renewal pathway and undergo several mitotic cell divisions to produce A_{pr} and A_{al} spermatogonia, which then differentiate without mitotic division into A_1 spermatogonia. The A_1 spermatogonia undergo another series of mitotic divisions that lead to the successive formation of A_2, A_3, A_4, In, and Type B spermatogonia. Thereafter, Type B spermatogonia divide to form preleptotene spermatocytes that enter meiosis to yield haploid spermatids, which then undergo spermiogenesis, leading to the production of spermatozoa.[1]

As a classical signaling molecule and a master regulatory protein kinase, MTOR can regulate a diverse array of cellular processes, such as growth, proliferation, differentiation, and metabolism, by forming two structurally and functionally distinct protein complexes termed mTOR complex 1 (mTORC1) and mTOR complex 2 (mTORC2).[8–13] In the clinical setting, MTORC1 plays a pivotal role in maintaining male reproductive health, and disrupted MTORC1 function impairs spermatogenesis, resulting in oligozoospermia or azoospermia and male sterility.[14–17] By studying distinct mouse models, several groups showed that mTORC1 can affect spermatogenesis and male fertility by regulating spermatogonial development.[18–20] For example, Busada *et al.*[18] reported that *in vivo* inhibition of mTORC1 by rapamycin blocks spermatogonial proliferation and differentiation. Two other groups found that germ cell-specific deletion of tuberous sclerosis 1 (TSC1) and tuberous sclerosis 2 (TSC2), two upstream inhibitors of mTORC1, both cause excessive differentiation of spermatogonia at the expense of their self-renewal.[19,20] These findings indirectly suggested that, as a core component of mTORC1, MTOR itself may be involved

[1]State Key Laboratory of Molecular Biology, Shanghai Key Laboratory of Molecular Andrology, CAS Center for Excellence in Molecular Cell Science, Shanghai Institute of Biochemistry and Cell Biology, Chinese Academy of Sciences, University of Chinese Academy of Sciences, Shanghai 200031, China; [2]State Key Laboratory of Cell Biology, Shanghai Key Laboratory of Molecular Andrology, CAS Center for Excellence in Molecular Cell Science, Shanghai Institute of Biochemistry and Cell Biology, Chinese Academy of Sciences, University of Chinese Academy of Sciences, Shanghai 200031, China.
Correspondence: Dr. YC Zhou (zhouych@sibcb.ac.cn) or Dr. YP Li (yipingli@sibcb.ac.cn)
Received: 12 August 2018; Accepted: 08 January 2019

in specific processes of spermatogonial development. In this study, we used stimulated by retinoic acid gene 8 (*Stra8*)-Cre to generate a germ cell-specific *Mtor* knockout (KO) mouse model to investigate the role of MTOR in spermatogonial development and male fertility.

MATERIALS AND METHODS

Animals

All animals used in our study were housed under a controlled lighting regime (14 h light; 10 h darkness) at 21°C–22°C with freely available food and water. Animal procedures were all approved by the Institutional Animal Care and Use Committee at the Shanghai Institute of Biochemistry and Cell Biology, Chinese Academy of Sciences (Shanghai, China). To generate germ cell-specific *Mtor* KO mice, male *Stra8*-Cre mice (No. 008208, The Jackson Laboratory) were crossed with female *Mtor*-floxed mice ($Mtor^{fl}$, No. 011009, The Jackson Laboratory) to generate $Mtor^{fl/+}$; *Stra8*-Cre male mice. Then, $Mtor^{fl/+}$; *Stra8*-Cre male mice were crossed with female $Mtor^{fl/fl}$ mice to produce $Mtor^{fl/\Delta}$; *Stra8*-Cre male mice, which we designated as *Mtor* KO mice. The $Mtor^{fl/+}$; *Stra8*-Cre male littermates were used as controls. Genomic DNA (gDNA) isolated from tail biopsies was used for PCR-based genotyping and primers for identifying Cre and floxed *Mtor* alleles were designed as described previously.[21–24] Wild-type (WT) C57BL/6J female mice were purchased from the Animal Center of the Chinese Academy of Sciences (Shanghai, China).

Testicular morphological analysis and sperm counts

Testes were collected immediately after the animals were killed. Whole body weights and testicular weights were measured on a chemical balance. Images of testes were recorded with a stereoscopic microscope (MVX10, Olympus, Shinjuku, Tokyo, Japan). Mature spermatozoa were collected from the cauda epididymidis and counted in a computer-assisted semen analysis (CASA) machine (HTM-TOX IVOS sperm motility analyzer, Animal Motility, version 12.3A, Hamilton Thorne Research, Beverly, MA, USA) as described previously.[25]

Fertility test

To evaluate the fertility of male mice, five *Mtor* KO mice and their littermate controls were mated with WT C57 female mice at a ratio of 1:2, starting at 8 weeks of age. The duration of the fertility test was 4 months and the C57 female mice were replaced each month. Successful conception was defined by the presence of a vaginal plug and a subsequent visibly growing abdomen. Cages were monitored daily and litter sizes were recorded at delivery.[20]

BrdU labeling

The BrdU labeling was done as described previously.[26] Briefly, mice were injected intraperitoneally with BrdU (50 μg g^{-1} body weight, B5002, Sigma-Aldrich, St. Louis, MO, USA) in phosphate-buffered saline (PBS), then killed 2 h later. Testes were collected and fixed in 4% paraformaldehyde (PFA)/PBS solution.

Histology, immunohistochemistry (IHC), and indirect immunofluorescence (IIF)

Histological and immunohistochemical analyses were performed as previously described with slight modifications.[26] Briefly, for histological analysis, mouse testes were fixed overnight in Bouin's fixative, dehydrated with graded ethanol, paraffin-embedded, and sectioned at 5 μm. The sections were then deparaffinized, rehydrated, and stained with hematoxylin and eosin (H&E). For immunohistochemical analysis, mouse testes were fixed overnight at 4°C in 4% PFA, dehydrated with graded ethanol, paraffin-embedded, and sectioned at 5 μm. The sections were deparaffinized, rehydrated, subjected to antigen retrieval by boiling in 0.01 mol l^{-1} sodium citrate buffer, pH 6.0 for 30 min, and cooled to room temperature. The sections were blocked with 10% donkey serum in PBS for 60 min at room temperature. Primary antibodies were diluted in blocking solution and added to the sections for overnight incubation at 4°C. For colorimetric detection, the samples were washed three times with PBS, incubated for 1 h at room temperature with appropriate biotinylated secondary antibodies, and developed using a DAB substrate kit (GK500705, Gene Tech Co. Ltd., Shanghai, China). The samples were then counterstained with hematoxylin, dehydrated, and mounted with neutral balsam. For fluorescence detection, corresponding fluorescence-conjugated secondary antibodies were added to the washed sections and incubated for 2 h at room temperature. The sections were then incubated with DAPI (2 μg ml^{-1}) for 5 min, washed three times with PBS, and mounted with fluorescent mounting medium (S3023, Dako North America Inc., Carpinteria, CA, USA). Primary antibodies used are listed in **Supplementary Table 1**. The sections were examined with an Olympus BX-51 microscope.

Cell quantification of IIF

For cell quantification, we counted the total number of germ cells positive for each marker in approximately 70 seminiferous tubules across distinct microscopic fields of the testicular sections. Total germ cell numbers were then divided by the numbers of seminiferous tubules to evaluate the relative population size of each subset of germ cells.

Statistics

For all statistical analyses, at least three biological replicates were taken. Data were analyzed by Prism Version 7.0a (GraphPad Software Inc., San Diego, CA, USA) and expressed as the mean ± standard deviation. Assessment of statistical significance was performed with the unpaired *t*-test. *P* values are indicated as follows: $^{*}P < 0.05$; $^{**}P < 0.01$; $^{***}P < 0.001$; $^{****}P < 0.0001$; not significant (NS) as $P > 0.05$.

RESULTS

Generation of germ cell-specific Mtor KO mice

We generated germ cell-specific *Mtor* KO mice by utilizing *Stra8*-Cre-mediated gene deletion. *Stra8*-Cre is initially expressed at postnatal day 3 (P3) in a subset of undifferentiated spermatogonia and is detected through to preleptotene stage spermatocytes,[24] so it is expected to direct floxed gene deletion in a substantial fraction of undifferentiated spermatogonia as well as differentiating spermatogonia and early meiotic spermatocytes.[19] To assess the efficacy of *Stra8*-Cre-driven *Mtor* deletion, we first crossed $Mtor^{F/+}$; *Stra8*-Cre male mice with WT female mice and analyzed the genotypes of their offspring (**Supplementary Figure 1**). Our results indicated that the recombination and excision efficiency of the floxed *Mtor* allele was up to 98% (**Table 1**). Then, we performed immunohistochemistry (IHC) on testicular sections with an antibody against MTOR. A marked decrease in MTOR-positive ($MTOR^{+}$) germ cells was found in the testes of *Mtor* KO mice (**Figure 1a**, **1a'**, **1b**, **1b'** and **Supplementary Figure 2**). Thereafter, we costained MTOR with promyelocytic leukemia zinc finger (PLZF, also known as zinc finger and BTB domain containing 16, ZBTB16), a widely used marker for undifferentiated spermatogonia.[27–30] Costaining found that while essentially all the PLZF-expressing cells were also positive for MTOR in the testes of control mice at postnatal day 7 (P7) and postnatal day 14 (P14), a large proportion (approximately 50% at P7 and approximately 60% at P14) of PLZF-positive ($PLZF^{+}$) cells were devoid of MTOR expression in the testes of *Mtor* KO mice at the same ages (**Figure 1c–1h**, **1c'–1h'** and **1i–1j**). In addition, costaining of MTOR with GFRA1, a more

Table 1: Quantitative data of genotyping and calculation of *Mtor* deletion efficiency

	Number of all pups	*Number of $Mtor^{fl/+}$ pups (number fl)*	*Number of $Mtor^{\Delta/+}$ pups (number Δ)*
Male 1	39	1	21
Male 2	33	0	16
Male 3	34	1	16
Male 4	32	0	16
Male 5	39	0	19
Male 6	43	1	18
Male 7	29	0	14
Total	249	3	120
Efficiency of *Mtor* deletion (number Δ/[number fl+number Δ] × 100%)	98%		

+: WT allele; fl: floxed allele; Δ: truncated allele

restricted marker for undifferentiated spermatogonia,[19,31–33] showed that the proportion of GFRA1$^+$/MTOR$^+$ germ cells were also significantly reduced (approximately 15% reduction at P7 and approximately 30% reduction at P14) in *Mtor* KO testes (**Supplementary Figure 3**). Taken together, these data demonstrate that *Stra8*-Cre successfully deleted *Mtor* in our KO mouse model and this germ cell-specific deletion was initiated in a subset of undifferentiated spermatogonia.

***Mtor* KO mice progressively lose their germ cells and fertility with age**

With *Stra8*-Cre-driven *Mtor* deletion confirmed, we then examined its influence on testicular development. Gross morphological observation showed that the testicular size of *Mtor* KO mice was only slightly reduced compared with control mice within the first 3 weeks after birth, but ceased to increase at about 5 weeks of age, and then progressively declined with age compared with the testicular size of control mice (**Figure 2a**). Detailed statistical analysis of the relative testis weight (testis weight to body weight ratio) further supported this finding (**Figure 2b**). We speculate that the age-related reduction in testicular size and weight was caused by a continual loss of germ cells and thus conducted histological analyses on testicular sections from *Mtor* KO and control mice at different ages. H and E staining revealed an apparent decrease of germ cells in the testes of *Mtor* KO mice as early as 2 weeks of age and a reduction in the lumen of seminiferous tubules (**Figure 2c** and **Supplementary Figure 4**). Moreover, some of the seminiferous tubules of *Mtor* KO mice eventually became vacuolated, which started at about 8–12 weeks of age and gradually spread throughout the whole testis with age (**Figure 2c**). Consistent with findings in the testis, H and E staining of epididymal sections showed vacuolation. Although a considerable number of mature spermatozoa were present in the cauda epididymidis of *Mtor* KO mice at 8–12 weeks of age, they were fewer than those of control mice and were lost quickly with age. We found no spermatozoa in the cauda epididymidis of *Mtor* KO mice starting from 24 weeks of age (**Figure 2d**). Our computer-assisted semen analysis (CASA)-based data also supported this result (**Figure 2e**). To evaluate the effect of this age-dependent loss of germ cells on fertility, each male at 8 weeks of age was housed with two WT females for a period of 4 months, during which the WT females were replaced by two new ones each month. The control males bred normally throughout the test period; however, *Mtor* KO males exhibited a progressive loss of fertility, displaying a similar trend to the loss of mature spermatozoa (**Figure 2f**). Altogether, these results indicate that *Mtor* deletion disrupts testicular development and causes a progressive loss of germ cells in and fertility of male mice.

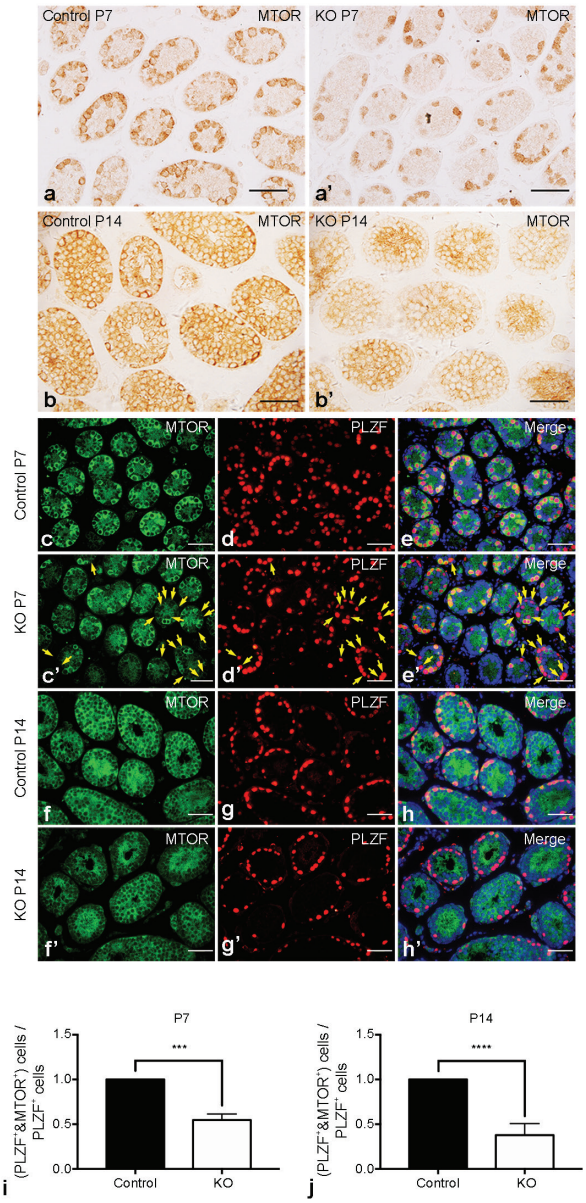

Figure 1: Verification of MTOR deletion in *Mtor* KO testes. Representative images of IHC for MTOR in the testes of postnatal day 7 (P7) (**a**) control and (**a'**) *Mtor* KO mice. Representative images of IHC for MTOR in the testes of postnatal day 14 (P14) (**b**) control and (**b'**) *Mtor* KO mice. Scale bar = 50 μm. Representative images of indirect immunofluorescence (IIF) for (**c**) MTOR and (**d**) PLZF, and (**e**) their merged images with DAPI (blue) in the testes of P7 control mice. Representative images of IIF for (**c'**) MTOR and (**d'**) PLZF, and (**e'**) their merged images with DAPI (blue) in the testes of P7 *Mtor* KO mice. Golden arrows indicate PLZF-positive cells with no MTOR expression. Representative images of IIF for (**f**) MTOR and (**g**) PLZF, and (**h**) their merged images with DAPI (blue) in the testes of P14 control mice. Representative images of IIF for (**f'**) MTOR and (**g'**) PLZF, and (**h'**) their merged images with DAPI (blue) in the testes of P14 *Mtor* KO mice. Scale bar = 50 μm. Quantification of the proportion of PLZF$^+$/MTOR$^+$ germ cells in the testes of (**i**) P7 and (**j**) P14 control and *Mtor* KO mice. IHC: immunohistochemistry. $^{***}P < 0.001$; $^{****}P < 0.0001$.

Spermatogonial differentiation in P7 Mtor KO testes

As mentioned above, *Mtor* deletion mediated by *Stra8*-Cre started in a subset of undifferentiated spermatogonia, so it was very likely to exert some influence on the biological functions of spermatogonia. To confirm this presumption, we assessed the cellular composition of

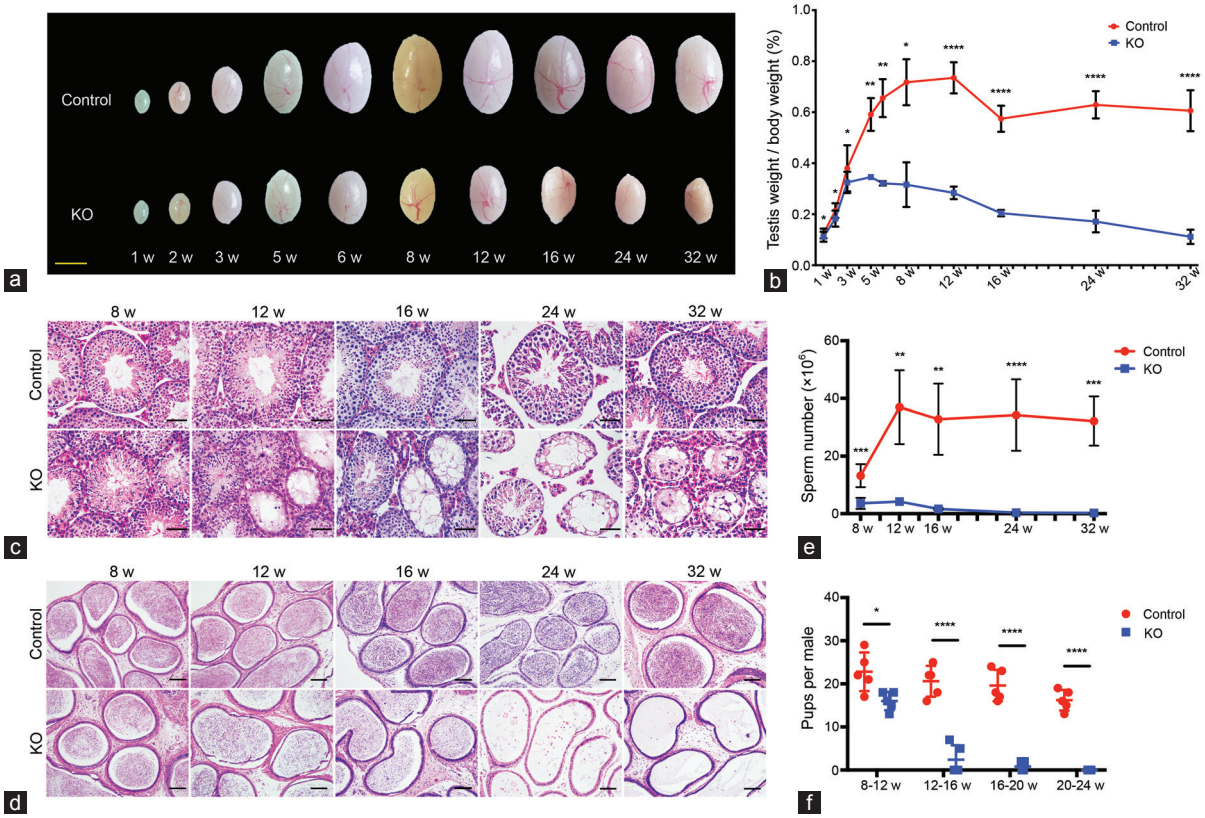

Figure 2: *Mtor* KO mice progressively lose their germ cells and fertility with age. (**a**) Representative images of testes from control and *Mtor* KO mice aged from 1 to 32 weeks old. Scale bar = 3mm. (**b**) Quantification of testis weight to body weight ratios of control and *Mtor* KO mice at different ages. (**c**) Representative images of H and E-stained testicular sections of control and *Mtor* KO mice aged from 8 weeks to 32 weeks old. Scale bars = 50 μm. (**d**) Representative images of H and E-stained cauda epididymal sections of control and *Mtor* KO mice at different ages. Scale bars = 100 μm. (**e**) Quantification of spermatozoa collected from the cauda epididymidis of control and *Mtor* KO mice at different ages. (**f**) Statistical analysis of the fertility of control and *Mtor* KO male mice at distinct age intervals. H and E: hematoxylin and eosin. $^{*}P < 0.05$; $^{**}P < 0.01$; $^{***}P < 0.001$; $^{****}P < 0.0001$.

testes from *Mtor* KO and control mice at P7, a time when the germ cells are mostly spermatogonia at different developmental stages.[34] We performed immunofluorescence analysis with the germ cell marker DDX4 and the Sertoli cell marker GATA4 and found fewer DDX4-positive (DDX4^{+}) germ cells in *Mtor* KO testes compared with control testes (**Figure 3a–3c**, **3a'–3c'** and **3p**), but no significant alteration in the number of GATA4-positive (GATA4^{+}) Sertoli cells (**Figure 3d–3f**, **3d'–3f'** and **3q**). To determine the identity of the germ cells that were affected by *Mtor* deletion, we continued immunostaining with several molecular markers differentially expressed in distinct germ cell subpopulations to assess the population size of each subset of germ cells. We stained testicular sections with an antibody against glial cell line derived neurotrophic factor family receptor alpha 1 (GFRA1), which is abundantly and selectively expressed in a restricted population of undifferentiated spermatogonia.[19,31–33] We found that the *Mtor* KO mice had an equal number of GFRA1-positive (GFRA1^{+}) germ cells to that of control mice (**Figure 3g–3i**, **3g'–3i'** and **3r**). Then, costaining of PLZF with KIT proto-oncogene receptor tyrosine kinase (KIT), a bona fide marker for differentiating spermatogonia,[35–37] revealed that the number of germ cells positive for PLZF but negative for KIT (PLZF^{+}/KIT^{-}) was not changed, but germ cells positive for both PLZF and KIT (PLZF^{+}/KIT^{+}) were markedly reduced in the testes of P7 *Mtor* KO compared with control mice (**Figure 3j–3l**, **3j'–3l'** and **3s**). Similarly, we also detected a reduced number of germ cells expressing STRA8 (**Figure 3m–3o**, **3m'–3o'** and **3t**), a differentiation marker mainly expressed in differentiating spermatogonia as well as preleptotene spermatocytes.[26,38–40]

Spermatogonial proliferation in P7 Mtor KO testes

As an apparent defect in spermatogonial differentiation was detected, we investigated whether spermatogonial proliferation was also affected by *Mtor* deletion. We costained GFRA1, PLZF, and STRA8 with the proliferation marker KI67 or BrdU to assess the proliferation status of distinct subsets of spermatogonia. We found that the proliferation rate of GFRA1^{+} spermatogonia was not changed (**Figure 4a**, **4a'** and **4d**); however, the proportion of PLZF^{+}/BrdU^{+} (**Figure 4b**, **4b'** and **4e**) and STRA8^{+}/BrdU^{+} (**Figure 4c**, **4c'** and **4f**) germ cells were both decreased in P7 *Mtor* KO mice.

Spermatogonial proliferation and differentiation in adult Mtor KO mice at 8 months of age

To evaluate the long-term impact of *Mtor* deletion on the normal function of spermatogonia, we assessed the population size of different subsets of spermatogonia in the testes of adult *Mtor* KO mice at 8 months of age, an age when the seminiferous tubules all became vacuolated. We detected no KIT^{+} differentiating spermatogonia in the testes of 8-month-old *Mtor* KO mice (**Figure 5a** and **5a'**), but PLZF^{+} undifferentiated spermatogonia were easily found (**Figure 5b** and **5b'**). In addition, quantitative analysis revealed that the number of PLZF^{+} germ cells was markedly decreased (**Figure 5c**). Costaining of PLZF with BrdU showed that the proportion of PLZF^{+}/BrdU^{+} germ cells also declined in *Mtor* KO mice (**Figure 5d**).

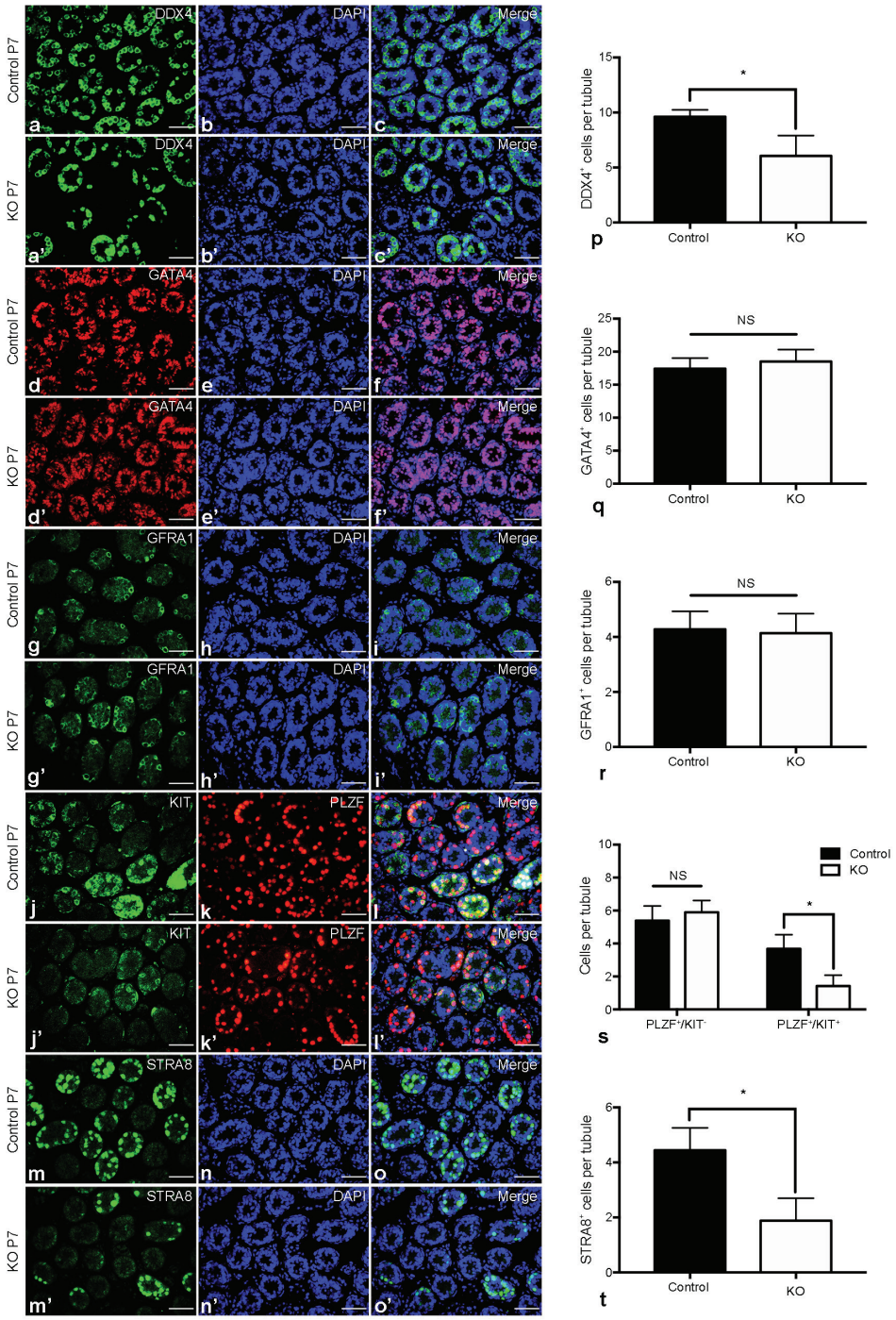

Figure 3: Spermatogonial differentiation in P7 *Mtor* KO testes. Representative images of indirect immunofluorescence (IIF) for (**a**) DDX4 and (**b**) DAPI, and (**c**) their merged images in the testes of P7 control mice. Representative images of IIF for (**a'**) DDX4 and (**b'**) DAPI, and (**c'**) their merged images in the testes of P7 *Mtor* KO mice. Representative images of IIF for (**d**) GATA4 and (**e**) DAPI, and (**f**) their merged images in the testes of P7 control mice. Representative images of IIF for (**d'**) GATA4 and (**e'**) DAPI, and (**f'**) their merged images in the testes of P7 *Mtor* KO mice. Representative images of IIF for (**g**) GFRA1 and (**h**) DAPI, and (**i**) their merged images in the testes of P7 control mice. Representative images of IIF for (**g'**) GFRA1 and (**h'**) DAPI, and (**i'**) their merged images in the testes of P7 *Mtor* KO mice. Representative images of IIF for (**j**) KIT and (**k**) PLZF, and (**l**) their merged images with DAPI (blue) in the testes of P7 control mice. Representative images of IIF for (**j'**) KIT and (**k'**) PLZF, and (**l'**) their merged images with DAPI (blue) in the testes of P7 *Mtor* KO mice. Representative images of IIF for (**m**) STRA8 and (**n**) DAPI, and (**o**) their merged images in the testes of P7 control mice. Representative images of IIF for (**m'**) STRA8 and (**n'**) DAPI, and (**o'**) their merged images in the testes of P7 *Mtor* KO mice. Scale bar = 50 μm. Quantification of (**p**) DDX4$^+$, (**q**) GATA4$^+$, (**r**) GFRA1$^+$, (**s**) PLZF$^+$/KIT$^-$, PLZF$^+$/KIT$^+$ and (**t**) STRA8$^+$ germ cells in the testes of P7 control and *Mtor* KO mice. $^*P < 0.05$.

DISCUSSION

Spermatogonial development is a vital prerequisite for spermatogenesis, and considerable research has been devoted to unraveling the details and exact mechanisms underlying the development of spermatogonia, including SSC self-renewal, spermatogonial proliferation, and spermatogonial differentiation. In the current study, we used *Stra8*-Cre

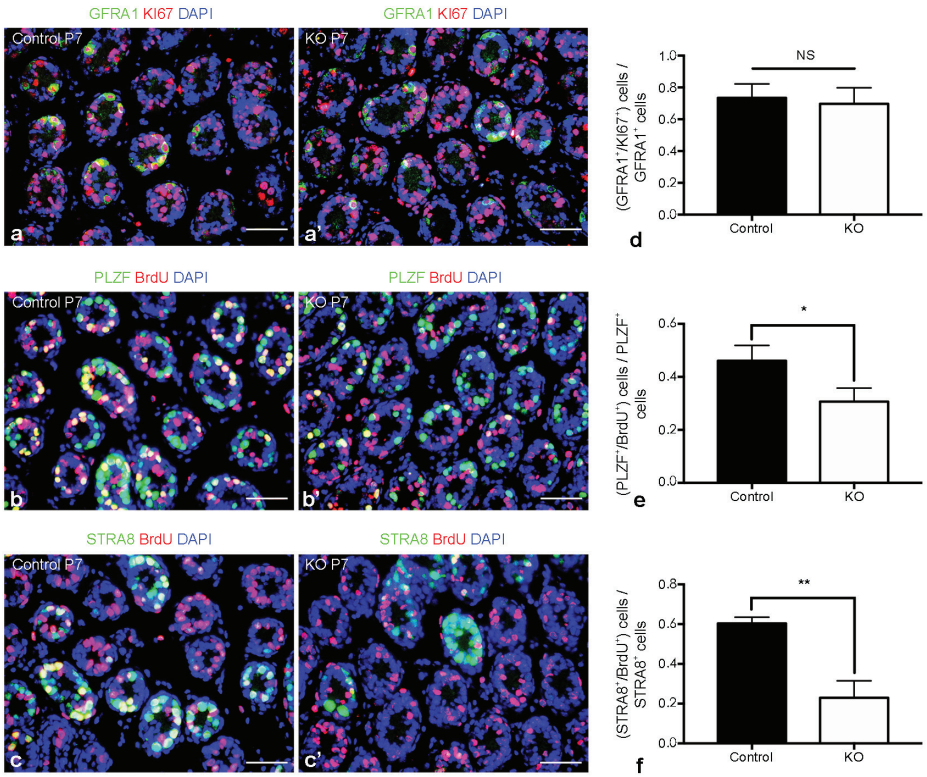

Figure 4: Spermatogonial proliferation in P7 *Mtor* KO testes. Representative images of costained GFRA1 (green), KI67 (red) and DAPI (blue) in the testes of P7 (**a**) control and (**a'**) *Mtor* KO mice. Representative images of costained PLZF (green), BrdU (red) and DAPI (blue) in the testes of P7 (**b**) control and (**b'**) *Mtor* KO mice. Representative images of costained STRA8 (green), BrdU (red) and DAPI (blue) in the testes of P7 (**c**) control and (**c'**) *Mtor* KO mice. Scale bars = 50 μm. Quantification of the proportion of (**d**) GFRA1$^+$/KI67$^+$, (**e**) PLZF$^+$/BrdU$^+$ and (**f**) STRA8$^+$/BrdU$^+$ germ cells in the testes of P7 control and *Mtor* KO mice. $^*P < 0.05$; $^{**}P < 0.01$.

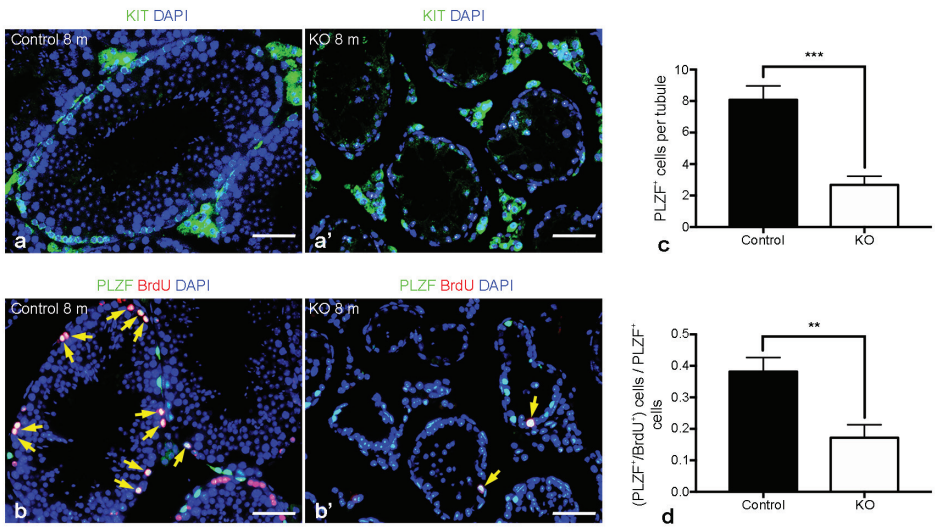

Figure 5: Spermatogonial proliferation and differentiation in adult *Mtor* KO mice at 8 months of age. Representative images of costained KIT (green) and DAPI (blue) in the testes of 8-month-old (**a**) control and (**a'**) *Mtor* KO mice. Representative images of costained PLZF (green), BrdU (red) and DAPI (blue) in the testes of 8-month-old (**b**) control and (**b'**) *Mtor* KO mice. Golden arrows indicate PLZF$^+$/BrdU$^+$ germ cells. Scale bars = 50 μm. (**c**) Quantification of PLZF$^+$ germ cells in the testes of 8-month-old control and *Mtor* KO mice. (**d**) Quantification of the proportion of PLZF$^+$/BrdU$^+$ germ cells in the testes of 8-month-old control and *Mtor* KO mice. $^{**}P < 0.01$; $^{***}P < 0.001$.

to generate a germ cell-specific *Mtor* KO mouse model to investigate the role of MTOR in spermatogonial development. Our results indicate that MTOR is required for spermatogonial proliferation and differentiation. When MTOR was deleted, the transition from undifferentiated to differentiating spermatogonia was greatly inhibited, leading to a marked reduction of differentiating spermatogonia. Moreover, MTOR deficiency also impeded the proliferation of spermatogonia, which further diminished the spermatogonia pool as well as the whole germ cell population. These outcomes are consistent with several previous studies. For instance, previous studies reported that mTORC1 is

involved in RA-induced translation of several genes required for spermatogonial proliferation and differentiation, and inhibition of mTORC1 activity by rapamycin severely suppresses spermatogonial proliferation and differentiation.[18,41] Toward the end of our study, these researchers published work in which they ablated *Mtor* more thoroughly in male germ cells using *Ddx4*-Cre to explore its role in spermatogonial development.[42] According to their recent data, *Mtor* deletion greatly impeded the proliferation and differentiation of spermatogonia without disturbing their survival and self-renewal.[42] Another two groups created mouse KO models with male germ cell-specific deletion of two upstream inhibitors of mTORC1, TSC1 and TSC2. They found that the ablation of TSC1 and TSC2 caused hyperactivation of MTORC1 signaling and excessive differentiation of undifferentiated spermatogonia, an effect opposite to that caused by MTOR deletion or mTORC1 inhibition.[19,20] These results, together with our own findings, reveal that MTOR is indispensable for the proliferation and differentiation of spermatogonia, and mTORC1 activity seems to be positively correlated with the differentiation of spermatogonia.

Our current study found that all the phenotypes caused by *Stra8*-Cre-mediated *Mtor* deletion seemed to occur in an age-dependent manner. For instance, although our *Mtor* KO mice became sterile at about 6 months old, their fertility was only partially lost when they were young. Interestingly, the incomplete phenotype of young adults observed in our study was also found in the studies of TSC1 and TSC2 mentioned above.[19,20] In both studies, a mixture of normal-appearing seminiferous tubules were found adjacent to degenerating tubules in the testes of 8–9-week-old KO mice, even when TSC1 and TSC2 were more extensively ablated using *Ddx4*-Cre.[19,20] The deletion of TSC1 driven by *Ddx4*-Cre resulted in an approximately 60% decline in epididymal sperm number as well as a partial loss of fertility.[20] We had speculated that it might be an intrinsic property of MTOR (mTORC1) to affect spermatogonial development in a mild and progressive manner when its activity is either removed or excessively activated. However, our assumption was negated by recent work from the Geyer group, in which they abolished MTOR function earlier and more thoroughly using *Ddx4*-Cre and then detected a more complete phenotype.[42] Specifically, all seminiferous tubules in *Ddx4*-Cre-mediated *Mtor* KO mice contained vacuoles as early as P18 and not a single spermatozoon was found in the cauda epididymidis throughout the whole reproductive lifespan.[42] This research, combined with our results, indicates that either the timing or efficiency of *Mtor* deletion mediated by different Cre lines causes the variation of phenotypes between the two distinct *Mtor* KO mouse models. From our results, the recombination and excision efficiency of floxed *Mtor* allele was up to 98%, demonstrating that *Stra8*-Cre drove a nearly complete *Mtor* deletion within the male germline. As the possibility for inefficient *Mtor* deletion was excluded, it seems that the incomplete phenotype found in our study was caused by a delayed initiation of *Mtor* deletion driven by *Stra8*-Cre. *Stra8*-Cre is active in a particular subset of undifferentiated spermatogonia that have already obtained a high propensity for differentiation, but is inefficient in those still possessing high self-renewal potential,[19] so the *Stra8*-Cre-induced *Mtor* deletion within undifferentiated spermatogonia may start at a relatively late stage when a considerable amount of MTOR proteins were already expressed. As it takes time to degrade all residual MTOR proteins, some undifferentiated spermatogonia may escape the differentiation arrest caused by MTOR deficiency and maintain a few rounds of spermatogenesis for a limited period of time. We detected weak expression of MTOR proteins in the residual germ cells of *Mtor* KO mice at different ages, providing supportive evidence for this hypothesis. However, more comprehensive examinations are still needed to fully confirm this proposal.

AUTHOR CONTRIBUTIONS

JC participated in the design of the study, carried out the experiments, and drafted the manuscript. ZBL helped perform the animal experiments. YLZ and MHT contributed to the design of the study, helped interpret the data, and revised the manuscript. YCZ and YPL supervised the study, participated in its design and coordination, and revised the manuscript. All authors read and approved the final manuscript.

COMPETING INTERESTS

All authors declared no competing interests.

ACKNOWLEDGMENTS

We would like to thank Dr. Qiang Liu, Dr. Yanfei Ru, and Dr. Guangxin Yao for critical reading of this manuscript. We also want to thank Zimei Ni for mouse handling and Aihua Liu for technical assistance in immunohistochemical analysis. This work was supported by the Ministry of Science and Technology of the People's Republic of China (NO. 2014CB943103), the National Natural Science Foundation of China (No. 31671203 and NO. 31471104), and the Science and Technology Commission of Shanghai Municipality (NO. 17JC1420100).

Supplementary Information is linked to the online version of the paper on the *Asian Journal of Andrology* website.

REFERENCES

1 Oatley JA, Brinster RL. Regulation of spermatogonial stem cell self-renewal in mammals. *Annu Rev Cell Dev Bi* 2008; 24: 263–86.
2 De Rooij DG, Russell LD. All you wanted to know about spermatogonia but were afraid to ask. *J Androl* 2000; 21: 776–98.
3 Mecklenburg JM, Hermann BP. Mechanisms regulating spermatogonial differentiation. *Results Probl Cell Differ* 2016; 58: 253–87.
4 de Rooij DG. The nature and dynamics of spermatogonial stem cells. *Development* 2017; 144: 3022–30.
5 Kanatsu-Shinohara M, Shinohara T. Spermatogonial stem cell self-renewal and development. *Annu Rev Cell Dev Biol* 2013; 29: 163–87.
6 Lord T, Oatley JM. A revised Asingle model to explain stem cell dynamics in the mouse male germline. *Reproduction* 2017; 154: R55–64.
7 Yoshida S. Elucidating the identity and behavior of spermatogenic stem cells in the mouse testis. *Reproduction* 2012; 144: 293–302.
8 Cornu M, Albert V, Hall MN. mTOR in aging, metabolism, and cancer. *Curr Opin Genet Dev* 2013; 23: 53–62.
9 Guertin DA, Sabatini DM. Defining the role of mTOR in cancer. *Cancer Cell* 2007; 12: 9–22.
10 Laplante M, Sabatini DM. mTOR signaling at a glance. *J Cell Sci* 2009; 122: 3589–94.
11 Laplante M, Sabatini DM. mTOR signaling in growth control and disease. *Cell* 2012; 149: 274–93.
12 Wullschleger S, Loewith R, Hall MN. TOR signaling in growth and metabolism. *Cell* 2006; 124: 471–84.
13 Zoncu R, Efeyan A, Sabatini DM. mTOR: from growth signal integration to cancer, diabetes and ageing. *Nat Rev Mol Cell Bio* 2011; 12: 21–35.
14 Bererhi L, Flamant M, Martinez F, Karras A, Thervet E, *et al.* Rapamycin-induced oligospermia. *Transplantation* 2003; 76: 885–6.
15 Skrzypek J, Krause W. Azoospermia in a renal transplant recipient during sirolimus (rapamycin) treatment. *Andrologia* 2007; 39: 198–9.
16 Deutsch MA, Kaczmarek I, Huber S, Schmauss D, Beiras-Fernandez A, *et al.* Sirolimus-associated infertility: case report and literature review of possible mechanisms (vol 7, pg 2414, 2007). *Am J Transplant* 2008; 8: 472–6.
17 Zuber J, Anglicheau D, Elie C, Bererhi L, Timsit MO, *et al.* Sirolimus may reduce fertility in male renal transplant recipients. *Am J Transplant* 2008; 8: 1471–9.
18 Busada JT, Niedenberger BA, Velte EK, Keiper BD, Geyer CB. Mammalian target of rapamycin complex 1 (mTORC1) is required for mouse spermatogonial differentiation *in vivo*. *Dev Biol* 2015; 407: 90–102.
19 Hobbs RM, La HM, Makela JA, Kobayashi T, Noda T, *et al.* Distinct germline progenitor subsets defined through Tsc2-mTORC1 signaling. *EMBO Rep* 2015; 16: 467–80.
20 Wang CX, Wang ZL, Xiong Z, Dai HQ, Zou ZP, *et al.* mTORC1 activation promotes

spermatogonial differentiation and causes subfertility in mice. *Biol Reprod* 2016; 95: 97.
21 Gangloff YG, Mueller M, Dann SG, Svoboda P, Sticker M, *et al*. Disruption of the mouse mTOR gene leads to early postimplantation lethality and prohibits embryonic stem cell development. *Mol Cell Biol* 2004; 24: 9508–16.
22 Risson V, Mazelin L, Roceri M, Sanchez H, Moncollin V, *et al*. Muscle inactivation of mTOR causes metabolic and dystrophin defects leading to severe myopathy. *J Cell Biol* 2009; 187: 859–74.
23 Bao JQ, Ma HY, Schuster A, Lin YM, Yan W. Incomplete cre-mediated excision leads to phenotypic differences between Stra8-iCre; Mov10l1(lox/lox) and Stra8-iCre; Mov10l1(lox/) mice. *Genesis* 2013; 51: 481–90.
24 Sadate-Ngatchou PI, Payne CJ, Dearth AT, Braun RE. Cre recombinase activity specific to postnatal, premeiotic male germ cells in transgenic mice. *Genesis* 2008; 46: 738–42.
25 Zhou YC, Ru YF, Wang CM, Wang SL, Zhou ZM, *et al*. Tripeptidyl peptidase II regulates sperm function by modulating intracellular Ca^{2+} stores via the ryanodine receptor. *PLos One* 2013; 8: e66634.
26 Chen Y, Ma L, Hogarth C, Wei G, Griswold MD, *et al*. Retinoid signaling controls spermatogonial differentiation by regulating expression of replication-dependent core histone genes. *Development* 2016; 143: 1502–11.
27 Buaas FW, Kirsh AL, Sharma M, McLean DJ, Morris JL, *et al*. Plzf is required in adult male germ cells for stem cell self-renewal. *Nat Genet* 2004; 36: 647–52.
28 Costoya JA, Hobbs RM, Barna M, Cattoretti G, Manova K, *et al*. Essential role of Plzf in maintenance of spermatogonial stem cells. *Nat Genet* 2004; 36: 653–9.
29 Hobbs RM, Seandel M, Falciatori I, Rafii S, Pandolfi PP. Plzf regulates germline progenitor self-renewal by opposing mTORC1. *Cell* 2010; 142: 468–79.
30 Hobbs RM, Fagoonee S, Papa A, Webster K, Altruda F, *et al*. Functional antagonism between Sall4 and Plzf defines germline progenitors. *Cell Stem Cell* 2012; 10: 284–98.
31 Naughton CK, Jain S, Strickland AM, Gupta A, Milbrandt J. Glial cell-line derived neurotrophic factor-mediated RET signaling regulates spermatogonial stem cell fate. (vol 74, pg 314, 2006). *Biol Reprod* 2006; 75: 660.
32 Nakagawa T, Sharma M, Nabeshima Y, Braun RE, Yoshida S. Functional hierarchy and reversibility within the murine spermatogenic stem cell compartment. *Science* 2010; 328: 62–7.
33 Grasso M, Fuso A, Dovere L, De Rooij DG, Stefanini M, *et al*. Distribution of GFRA1-expressing spermatogonia in adult mouse testis. *Reproduction* 2012; 143: 325–32.
34 Bellve AR, Cavicchia JC, Millette CF, O'Brien DA, Bhatnagar YM, *et al*. Spermatogenic cells of the prepuberal mouse. Isolation and morphological characterization. *J Cell Biol* 1977; 74: 68–85.
35 Mithraprabhu S, Loveland KL. Control of KIT signalling in male germ cells: what can we learn from other systems? *Reproduction* 2009; 138: 743–57.
36 Niedenberger BA, Busada JT, Geyer CB. Marker expression reveals heterogeneity of spermatogonia in the neonatal mouse testis. *Reproduction* 2015; 149: 329–38.
37 Schrans-Stassen BH, Van de Kant HJ, De Rooij DG, Van Pelt AM. Differential expression of c-kit in mouse undifferentiated and differentiating type A spermatogonia. *Endocrinology* 1999; 140: 5894–900.
38 OuladAbdelghani M, Bouillet P, Decimo D, Gansmuller A, Heyberger S, *et al*. Characterization of a premeiotic germ cell-specific cytoplasmic protein encoded by Stra8, a novel retinoic acid-responsive gene. *J Cell Biol* 1996; 135: 469–77.
39 Zhou Q, Nie R, Li Y, Friel P, Mitchell D, *et al*. Expression of stimulated by retinoic acid gene 8 (Stra8) in spermatogenic cells induced by retinoic acid: an *in vivo* study in Vitamin A-sufficient postnatal murine testes. *Biol Reprod* 2008; 79: 35–42.
40 Endo T, Romer KA, Anderson EL, Baltus AE, de Rooij DG, *et al*. Periodic retinoic acid-STRA8 signaling intersects with periodic germ-cell competencies to regulate spermatogenesis. *Proc Natl Acad Sci U S A* 2015; 112: E2347–56.
41 Busada JT, Chappell VA, Niedenberger BA, Kaye EP, Keiper BD, *et al*. Retinoic acid regulates Kit translation during spermatogonial differentiation in the mouse. *Dev Biol* 2015; 397: 140–9.
42 Serra ND, Velte EK, Niedenberger BA, Kirsanov O, Geyer CB. Cell-autonomous requirement for mammalian target of rapamycin (Mtor) in spermatogonial proliferation and differentiation in the mouse. *Biol Reprod* 2017; 96: 816–28.

Supplementary Table 1: Antibodies for immunohistochemistry and indirect immunofluorescence

Protein	*Vendor (catalog number)*	*Clonality*	*Host species*	*Dilution*
MTOR	Cell signaling technology (#2983T)	Monoclonal	Rabbit	1:200
DDX4	Abcam (ab13840)	Polyclonal	Rabbit	1:500
GATA4	Santa Cruz (sc-25310)	Monoclonal	Mouse	1:500
GFRA1	R and D systems (AF560-SP)	Polyclonal	Goat	1:200
PLZF	Santa Cruz (sc-28319)	Monoclonal	Mouse	1:200
PLZF	Santa Cruz (sc-22839)	Polyclonal	Rabbit	1:200
KIT	Cell signaling technology (#3074S)	Monoclonal	Rabbit	1:50
KI67	Abcam (ab15580)	Polyclonal	Rabbit	1:200
BrdU	Millipore (05-633)	Monoclonal	Mouse	1:200

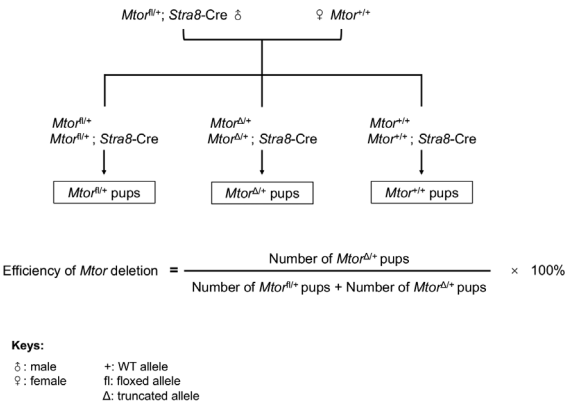

Supplementary Figure 1: Mating scheme for *Mtor* deletion efficiency assessment.

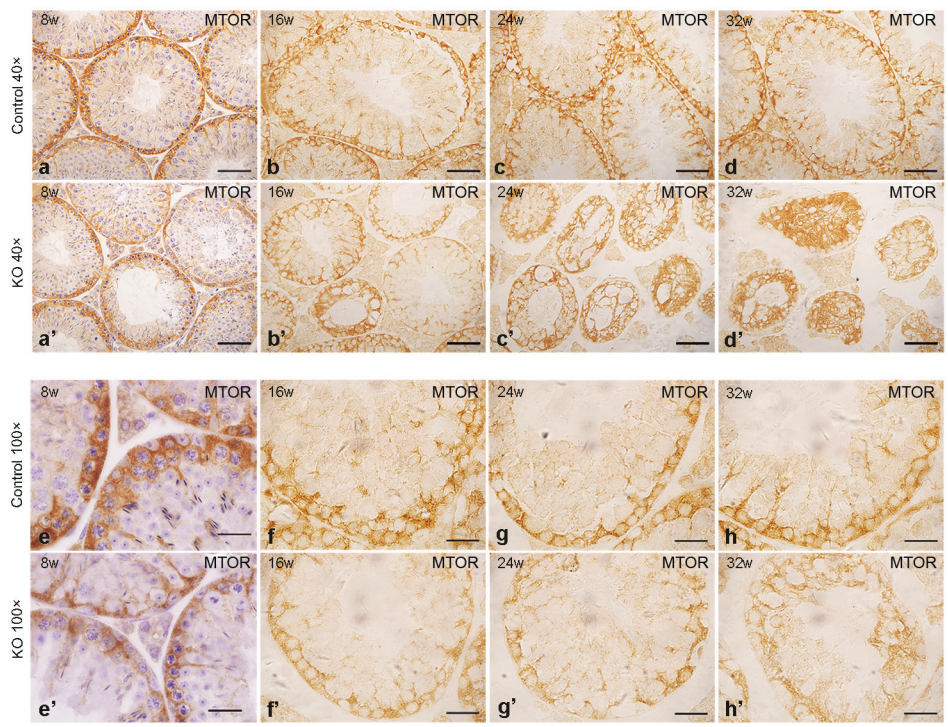

Supplementary Figure 2: Weak expression of MTOR proteins remained in the residual germ cells of *Mtor* KO mice. Representative ×40 images of IHC for MTOR in the testes of control mice at (**a**) 8 weeks, (**b**) 16 weeks, (**c**) 24 weeks and (**d**) 32 weeks of age. Representative ×40 images of IHC for MTOR in the testes *Mtor* KO mice at (**a'**) 8 weeks, (**b'**) 16 weeks, (**c'**) 24 weeks and (**d'**) 32 weeks of age. Bar = 50 µm. Representative ×100 images of IHC for MTOR in the testes of control mice at (**e**) 8 weeks, (**f**) 16 weeks, (**g**) 24 weeks and (**h**) 32 weeks of age. Representative ×100 images of IHC for MTOR in the testes *Mtor* KO mice at (**e'**) 8 weeks, (**f'**) 16 weeks, (**g'**) 24 weeks and (**h'**) 32 weeks of age. Bar = 20 µm. IHC: immunohistochemistry.

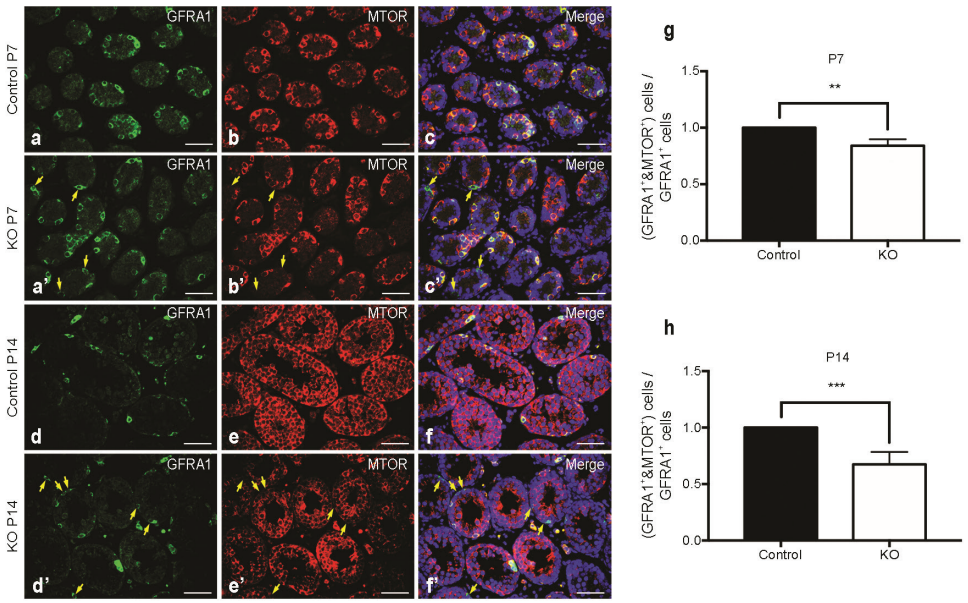

Supplementary Figure 3: Quantification of the efficiency of MTOR deletion in GFRA1$^+$ germ cells. Representative images of indirect IIF for (**a**) GFRA1 and (**b**) MTOR, and (**c**) their merged images with DAPI (blue) in the testes of postnatal day 7 (P7) control mice. Representative images of IIF for (**a'**) GFRA1 and (**b'**) MTOR, and (**c'**) their merged images with DAPI (blue) in the testes of P7 *Mtor* KO mice. Representative images of IIF for (**d**) GFRA1 and (**e**) MTOR, and (**f**) their merged images with DAPI (blue) in the testes of postnatal day 14 (P14) control mice. Representative images of IIF for (**d'**) GFRA1 and (**e'**) MTOR, and (**f'**) their merged images with DAPI (blue) in the testes of P14 *Mtor* KO mice. Bar = 50 μm. Golden arrows indicate GFRA1-positive cells with no MTOR expression. Quantification of the proportion of GFRA1$^+$/MTOR$^+$ germ cells in the testes of (**g**) P7 and (**h**) P14 control and *Mtor* KO mice. IIF: immunofluorescence. $^{**}P < 0.01$; $^{***}P < 0.001$.

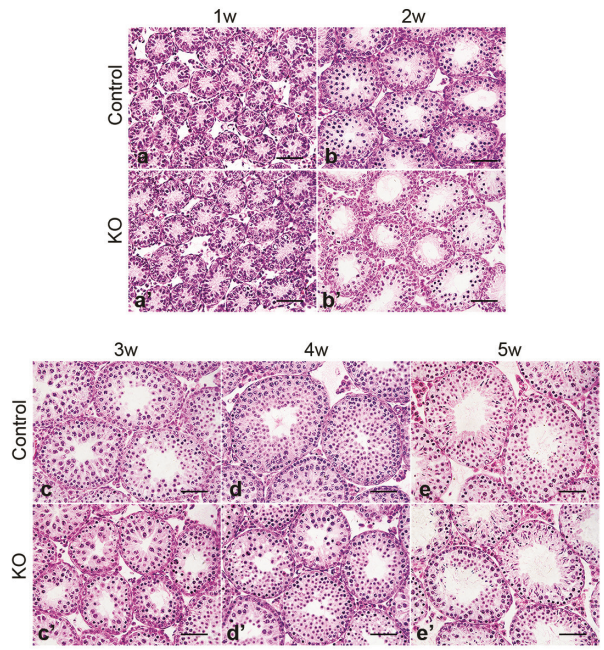

Supplementary Figure 4: An apparent loss of germ cells in the testes of *Mtor* KO mice found as early as 2 weeks of age. Representative images of H&E-stained testicular sections of control mice at (**a**) 1 week, (**b**) 2 weeks, (**c**) 3 weeks, (**d**) 4 weeks and (**e**) 5 weeks of age. Representative images of H&E-stained testicular sections of *Mtor* KO mice at (**a'**) 1 week, (**b'**) 2 weeks, (**c'**) 3 weeks, (**d'**) 4 weeks and (**e'**) 5 weeks of age. Bar = 50 μm.